Epochal Changes in ENSO–Streamflow Relationships in Sri Lanka

LAREEF ZUBAIR

International Research Institute for Climate and Society, Palisades, New York

JANAKI CHANDIMALA

Foundation for Environment, Climate, and Technology, Digana Village, Sri Lanka

(Manuscript received 17 October 2005, in final form 4 April 2006)

ABSTRACT

In an effort to use climate predictions for streamflow and malaria hazard prediction, the decadal variability of the El Niño–Southern Oscillation (ENSO) influence on streamflow and rainfall in the Kelani River in Sri Lanka was investigated based on records from 1925 to 1995. In the last half century, the warm ENSO phase was associated with decreased annual streamflow and the cold ENSO phase with increased streamflow. The annual streamflow had a negative correlation (warm ENSO associated with low streamflow) with the concurrent ENSO index of Niño-3.4 that was significant at the 5% level. This negative correlation with Niño-3.4 is enhanced to a 1% significance level if the aggregate streamflow from January to September alone is considered. There has been a transition in correlation between January–September streamflow and ENSO between the 1950s and 1970s from near or above zero to negative values that have 95% significance levels reminiscent of an epochal shift. This shift was evident when considering the period when the southwest monsoon dominates (April–September) or when correlations were undertaken between the seasonal streamflow and rainfall and the ENSO index in the month prior to each season. Since the relationship between ENSO and Sri Lankan streamflow has strengthened in recent decades the potential for ENSO-based prediction is retained. The epochal shift may also explain why malaria epidemics ceased to co-occur frequently with El Niño episodes after 1945.

1. Introduction

The El Niño–Southern Oscillation (ENSO) phenomenon is now recognized as a primary mode of seasonal climatic variability, particularly in the Tropics (Ropelewski and Halpert 1987). Sensitivity of streamflow to ENSO has been investigated for a number of rivers (Wang and Eltahir 1999; Whitaker et al. 2001; Dettinger et al. 2000). These relationships provide a basis to develop streamflow predictions to aid water resources management. The work reported here is part of such an effort in Sri Lanka where a significant ENSO influence has been identified (Rasmusson and Carpenter 1983; Ropelewski and Halpert 1987; Suppiah 1996).

The phases of the ENSO phenomena associated with anomalously (by at least 0.4°C) warm and cold sea surface in the equatorial eastern Pacific Ocean are referred to as El Niño and La Niña, respectively. During El Niño events, the modulations of climate in Sri Lanka are due to the alteration in intensity and location of the large-scale equatorial circulation system referred to as the Walker cell (Allan et al. 1996). During El Niño events, the rainfall is enhanced from October to December and diminished from January to March and July to August (Rasmusson and Carpenter 1983; Suppiah 1996; Zubair 2002a).

The ENSO-induced teleconnection is through large-scale east–west shifts in the "Walker circulation" of the Indo–Pacific regions. During an El Niño event, the tropical convection and the associated rising limb of the Walker circulation of the large-scale circulation normally located in the western Pacific shift toward the anomalously warm waters in the central and eastern Pacific. Consequently, there is an anomalous subsidence extending from the western Pacific to South Asia.

There has been an epochal shift in the ENSO and

Corresponding author address: Lareef Zubair, International Research Institute for Climate and Society, Lamont Campus, The Earth Institute at Columbia University, P.O. Box 1000, Palisades, NY 10964-8000.
E-mail: lareef@iri.columbia.edu

summer monsoon rainfall relationship during the 1950s in neighboring India (Kumar et al. 1999a). Epochal shifts can undermine statistical prediction schemes that are based on stationarity of historical data. In addition, the ENSO–monsoon rainfall relationship has weakened in the last decade (Kumar et al. 1999b). While Kumar et al. (1999b) held out the possibility that global warming may cause the weakening of the relationship, other explanations that have been proposed are that this weakening could be simply driven by decadal variation in the solar irradiance (Mehta and Lau 1997); that the interdecadal variation may be intrinsic to the coupled ocean–atmosphere mode (Krishnamurti and Goswami 2000); that it may be driven by decadal variations in the Atlantic circulation (Chang et al. 2001) and by decadal variations in the Indian Ocean Dipole (Ashok et al. 2001); or that this weakening may be attributed simply to stochasticity (Gershunov et al. 2001).

In this paper, the decadal variability of the ENSO influences on streamflow and rainfall in the Kelani catchment in Sri Lanka is investigated. The Kelani catchment rainfall is significantly affected by large-scale phenomenon. The low-level wind over South Asia is southwesterly during the boreal summer (Fig. 1a) and switches to northeasterly as the winter progresses, starting in October. During summer, rain falls all over South Asia, but is diminished over southern peninsular India and Sri Lanka (Fig. 1b). After October, the rainfall is enhanced over peninsular India, Sri Lanka, and the equatorial eastern Indian Ocean.

The Kelani River has one of the longest streamflow records in Sri Lanka. Its streamflow has a tremendous influence on hydroelectricity generation, flood risk, and water supply for the commercial capital city of Colombo. The Kelani originates at an altitude of 2400 m and garners rainfall on the western slopes of the central mountain ridge in the island. These slopes have the highest annual rainfall in the island with the annual precipitation varying between 2 and 5 m. The other major rivers in Sri Lanka, the Mahaweli, Walawe, and Kalu, also originate in the same region and have similar hydroclimatic characteristics.

Islandwide water allocation for agriculture is undertaken at the start of the planting season in April and October. Predictions that are available for April–September and October–March seasons shall be useful. Hydroelectricity reservoirs are drawn down from January until September with partial replenishment from the April–June rainfall. Thus predictions for January–September and April–September streamflow shall be useful for water management.

The decadal modulation of the ENSO relationship with streamflow and rainfall is also important on account of its effect on malaria hazard. El Niño episodes result in modulation of rainfall and streamflow leading to increased pooling suitable for mosquito breeding in river banks and in natural depressions (Bouma and Van der Kaay 1996). Malaria epidemics have occurred with significant frequency from 1880 to 1945 during El Niño episodes (Bouma and Van der Kaay 1996) but not in the next three decades. Decadal modulation of the ENSO influence on rainfall and streamflow could help unravel the causes of the decadal variations in ENSO influence on malaria.

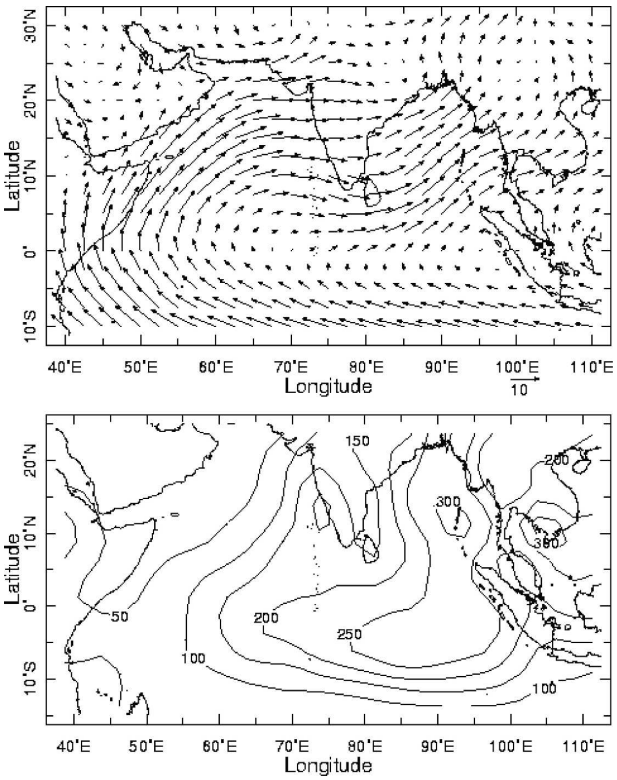

FIG. 1. (a) The mean low-level wind field at 925 mb from April to September for 1958–2002 (m s^{-1}). Data obtained from NCEP–NCAR reanalysis (Kistler et al. 2001). (b) The mean monthly rainfall during April–September for 1979 to 2004 (mm $month^{-1}$). Data obtained from the CAMS_OPI dataset (Janowiak and Xie 1999).

The objectives for this work are to characterize the ENSO–streamflow–rainfall relationships in Sri Lanka, to investigate whether epochal changes are evident in this relationship, and to assess the implications for hydroclimatic prediction.

2. Data and methods

a. ENSO data

The sea surface temperature (SST) index of Niño-3.4 was used as an index for ENSO. The Niño-3.4 index

was obtained by averaging the sea surface temperature anomalies (Kaplan et al. 1998) in the equatorial eastern Pacific Ocean (5°S–5°N, 120°–180°W).

Different ENSO indices (Southern Oscillation index, Niño-1, Niño-2, Niño-3, Niño-3.4, Niño-4) are able to capture the ENSO influences in different seasons with slightly different sensitivity (Hanley et al. 2003). SST-based indices in the central and eastern equatorial Pacific Ocean represent the ENSO response over the Asian monsoon (Soman and Slingo 1997). We have undertaken studies with other SST-based indices and the Southern Oscillation index, and these yield results that are similar to that based on Niño-3.4.

b. Streamflow data

The Kelani basin spans 2292 km^2. It is located within the western hill slopes discharging to the sea at Colombo on Sri Lanka's western coast. Of the total average annual rainfall of 8200 MCM (MCM = million cubic meters) in the entire Kelani basin, approximately 3300 MCM is discharged to the sea. Monthly streamflow records for the Kelani are available at 16 discharge measuring stations from the Sri Lanka Department of Irrigation. Of these records, the oldest record is at Nagalagam Street, Colombo (6°57′N, 79°52′E), commencing in 1924 and terminating in 1960. The Colombo gauging station is near the sea and has a catchment of 2085 km^2. The station that has the longest contemporary records is at the Glencourse Gorges [6°58′N, 80°10′E, 32 m above sea level (ASL)] where the Kelani descends to the lowlands of the island. Glencourse has a catchment of 1463 km^2 and streamflow records from 1948 to 1995. There is high correlation ($r = 0.93$) between the Glencourse and Colombo streamflow records during the period in which their records overlap (1948 to 1960). The data for Glencourse for the period from 1925 to 1948 was estimated based on a regression relationship calibrated for the overlapping period. We have compared the Glencourse streamflow data with those of stations both downstream and upstream as a check of extreme values.

Since 1953, the operation of two reservoirs at its headstream has modulated the Kelani streamflow. These reservoirs have a small storage of 169 MCM and a combined drainage basin area of only 10% of the Kelani basin. The impacts of reservoir management on hydroclimatic analysis were assumed to be minimal given that 90% of the Kelani basin is unregulated, and the fact that the storage capacity of these reservoirs are small.

c. Rainfall data

The Kelani catchment lies within a climatically homogeneous western hill slopes region as identified by Puvaneswaran and Smithson (1993). There are no Department of Meteorology stations within the upper Kelani catchment. However, there are 16 stations at government hospitals, railway stations, and tea estates that keep records (Zubair 2004). The rain gauges are provided by the Department of Meteorology, and the Department of Meteorology personnel inspect these gauges and undertake quality control of the data. We have undertaken quality tests for this data—identifications of outliers, cross checks for extreme values, checks for drifts in the data, and cross-correlation analysis. Based on this analysis, we decided to use only nine of these stations that had good coverage of the basin. A monthly catchment rainfall index was constructed for Glencourse by areally averaging rainfall observations of these rainfall stations.

We compared the results with monthly rainfall observations at three Sri Lanka Department of Meteorology/World Meteorological Organization (WMO) stations that are distributed in the wider western hill slopes region [Kandy (7°20′N, 80°38′E, 477 m ASL), Nuwara Eliya (6°58′N, 80°46′E, 1895 m ASL), and Ratnapura (6°40′N, 80°25′E, 34 m ASL)] (Fig. 2). A representative rainfall index for the western hill slopes (regional rainfall index) was constructed by averaging the rainfall of these stations. The catchment rainfall has a similar seasonality as the regional rainfall (Fig. 3a). The catchment rainfall is fractionally greater than the regional rainfall, as it is more compactly located in a region with the highest rainfall over Sri Lanka during the months from March to November.

d. Global circulation and rainfall

Circulation fields were obtained from the National Centers for Environmental Prediction–National Center for Atmospheric Research (NCEP–NCAR) reanalysis at monthly frequency from 1948 (Kistler et al. 2001). Global rainfall was obtained from the climate anomaly monitoring system – outgoing longwave radiation precipitation index (CAMS–OPI) monthly dataset (Janowiak and Xie 1999).

e. Correlation analysis

Correlation analysis was used to identify relationships between the monthly ENSO indices and streamflow or rainfall using Spearman's ranked correlation and with the Pearson algorithm (Press et al. 1992). The Spearman rank correlation is nonparametric and suited for non-Gaussian data. A correlation was taken to be significant when the hypothesis that there was no correlation between two time series was unlikely with a probability of 95%.

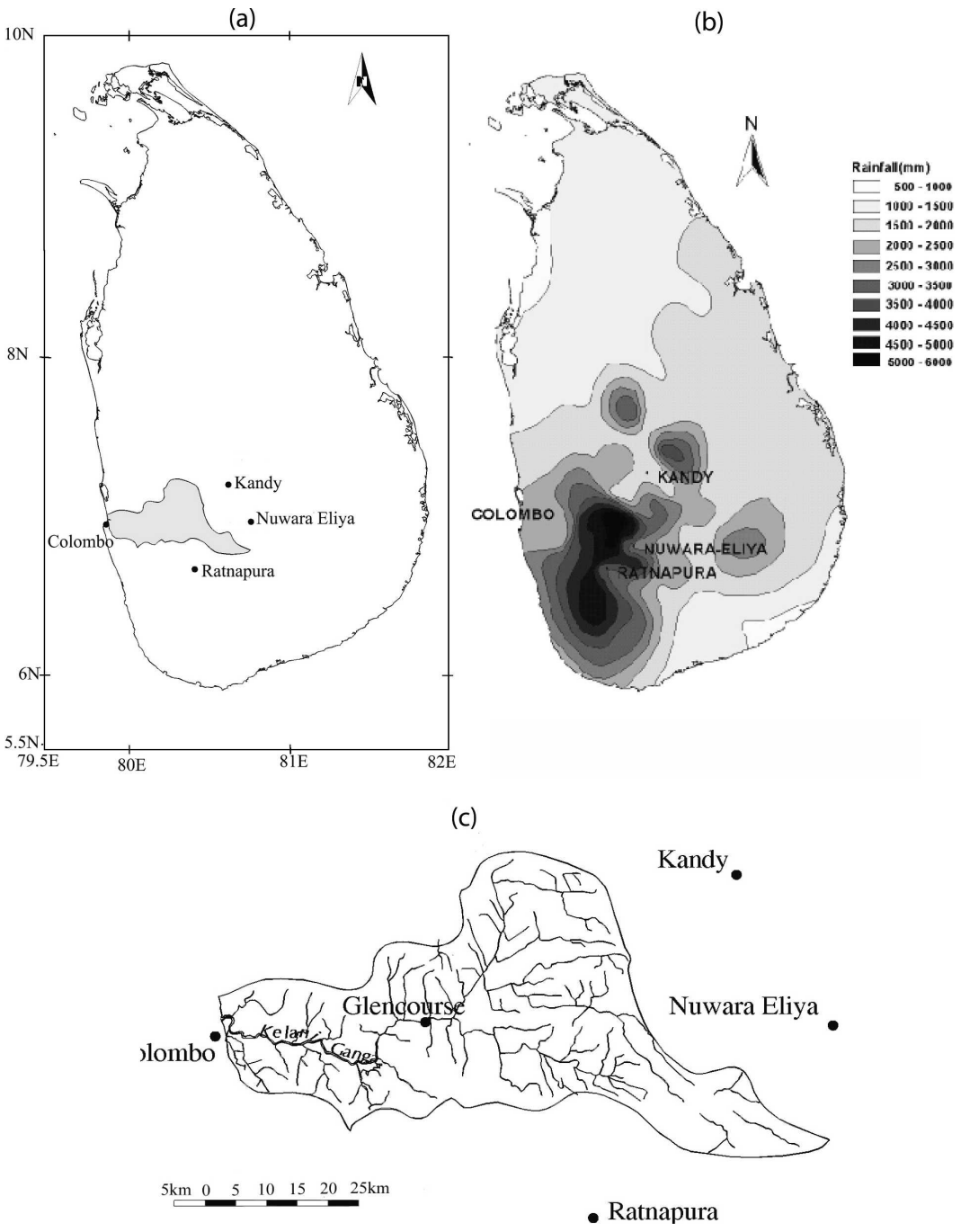

FIG. 2. (a) The Kelani basin is shaded within the location map for Sri Lanka. (b) Annual rainfall. (c) The streams and the streamflow measuring stations.

The evolution of correlations between variables was captured with windowed running correlations. To assess the sensitivity of the running correlations to window length, we considered three window lengths—15, 21, and 31 yr—but present only the running correlation for the 21-yr window while describing the results obtained with the other two window sizes. We followed the procedure attributed to Gershunov et al. (2001) to assess the statistical significance of decadal changes in running window correlations.

f. Nonstationarity

Nonstationarity in climate data could be due to low-frequency drifts, trends, discontinuities, outliers, and

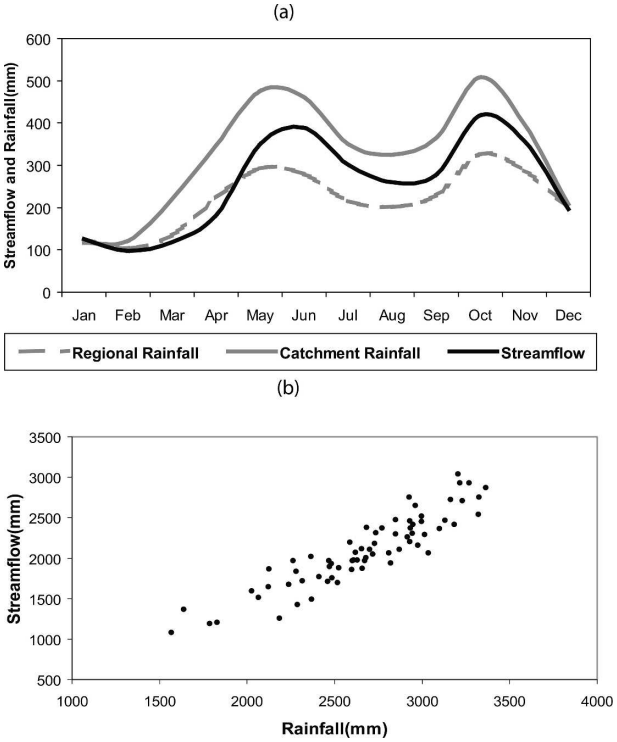

FIG. 3. (a) The climatology of western hills region rainfall, Glencourse catchment rainfall, and streamflow for the period 1925–95. (b) Scatterplots of the catchment streamflow vs rainfall for the April–September season.

random walks (Yaffee and McGee 2000). We have revisited outliers and checked these against time series in neighboring streamflow stations and rainfall indices for the catchment and the region. We verified that the results reported here on the decadal scale modulation of relationships between streamflow and ENSO were not due to trends and drifts by the use of alternative rainfall and streamflow datasets. We checked the influence of any low-frequency variability by repeating the diagnostics reported here after high-pass filtering. A high-pass Fourier filter with a Hamming window (Oppenheim and Schafer 1975) was implemented to remove features of wavelengths larger than approximately 100 months.

3. Results

a. Annual climatology

The rainfall climate of Sri Lanka is characterized by a bimodal distribution with peaks around May and September due to the passage of the intertropical convergence zone over the area during these times of the year (Fig. 3a). In addition, the monsoonal influences and cyclonic storms from the Bay of Bengal contribute to high rainfall from October to December. The western hill slopes also receive orographic rainfall from April to September when westerly winds prevail (Zubair 2002b). The Kelani catchment is on the windward side of the central mountain massif that rises to a height of approximately 2 km. Northeasterlies dominate from December to February and orographic rainfall leads to a slight diminishment of rainfall on the lee side, which includes the Kelani catchment.

The following aggregations of months have consistent ENSO influence: January–March, July–August, and October–December (Rasmusson and Carpenter 1983; Zubair 2002a). During April, June, and September the ENSO influences are ambiguous. For this analysis, the seasons were chosen on a quarterly basis, that is, January–March (JFM), April–June (AMJ), July–September (JAS), and October–December (OND): this choice maintains a consistent ENSO influence in each quarter and it relates to the planting and harvesting phases of the traditional agricultural seasons, *Yala* (April–September) and *Maha* (October–March).

b. Rainfall–streamflow relationships

Seasonal rainfall and streamflow values for January to September were tested for normality using the Kolmogorov–Smirnov test—in both cases the p values were too large to reject the null hypothesis of normality at a 99% confidence level. Computation of autocorrelations for streamflow and rainfall show that there are no significant lag relationships.

The rainfall–streamflow relationship has been largely robust during the period of record. The dispersion in the scatterplot between streamflow and rainfall is modest (Fig. 3b).

To understand if there is an influence on streamflow due to land-use changes or construction of small dams in the 1950s, we undertook running correlations between streamflow and rainfall for April–June and July–September. The results (Fig. 4a) show that there were no dramatic shifts in the rainfall–streamflow relationship in the record, and the correlation has been above 0.75 with improvement in the recent period. There was a slight drop in the correlations around the 1960s due to low-frequency drift in the streamflow calibration. Neighboring streamflow stations did not reproduce this trend and this drop was not replicated when correlations were conducted with high-pass-filtered data. The relationship between rainfall and streamflow is more consistent from April to September. The consistency between rainfall and streamflow also strengthen evidence for the quality of the datasets.

The streamflow is negatively correlated with ENSO for the three quarterly seasons from January to Sep-

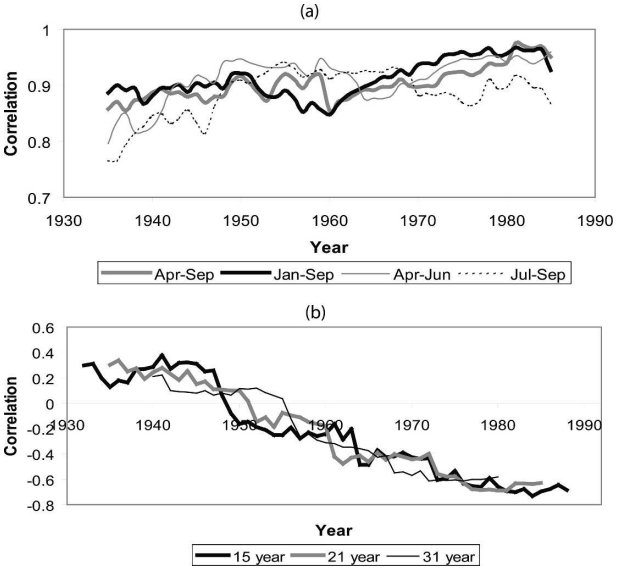

FIG. 4. (a) The running correlation with a 21-yr window between catchment streamflow and catchment rainfall at Glencourse for April–September, January–September, April–June, and July–September periods. (b) The 21-yr sliding window correlation between the concurrent April–September streamflow and Niño-3.4 is shown as a function of the central year of the window of sizes 15, 21, and 31 yr.

tember in the recent period. The correlation values between ENSO and October–December streamflow are positive and weak and it is not analyzed further. The January–September, April–September, and July–September aggregate streamflow have correlations from 1950 to 1995 of −0.55, −0.45, and −0.37, respectively, with contemporaneous Niño-3.4 that are all significant at the 1% level.

In contrast, the annual streamflow shows a weak positive correlation with Niño-3.4 before 1950 (Table 1). The January–September streamflow shows a weak positive correlation with Niño-3.4 before 1950 as well.

The decadal variability in ENSO–streamflow relationship is manifested by using a sliding windowed correlation of the contemporaneous Niño-3.4 and streamflow between January and September (Fig. 4b). In this and subsequent figures, the correlation for the window centered on a particular year is plotted against that year. This figure shows a drop in the correlation between streamflow and Niño-3.4 that is robust, consistent across window sizes of 15, 21, and 31 yr, and that is retained under high-pass filtering.

The correlation between streamflow and ENSO, which was positive in the 1930s, went through a transition around 1950 and turned negative (reaching −0.5) for January–September by 1960 (Fig. 5a). The transitions were retained for the catchment rainfall (Fig. 5a) and for high-pass-filtered versions of the rainfall and streamflow (Fig. 5b) and when correlations were conducted between the seasonal rainfall and streamflow indices with the previous Decembers' Niño-3.4 (Fig. 5c).

This transition was present but delayed until 1970 for the April–September season (Fig. 6a). The character of the transition was retained for high-pass-filtered versions of the rainfall and streamflow (Fig. 6b). The correlations between April–September rainfall and streamflow with the March Niño-3.4 showed a transition that was also significant but with some differences (Fig. 6c). The decline is from a high positive value of +0.5 to −0.4 during the recent period.

To assess the significance of the decadal shifts in running correlation, we used the tabulations of significance thresholds of standard deviations of running correlations as a function of running window width and correlation coefficient (Gershunov et al. 2001). As an example, consider the running correlation between streamflow and Niño-3.4 with a window of width 21 yr and mean correlation value of −0.21. The 5th and 95th percentile of the standard deviation of the variability due to stochasticity alone was estimated as 0.115 and 0.28, respectively. The standard deviation of the running correlation between January–September streamflow and Niño-3.4 for Glencourse was 0.34 (>0.28). Thus the decadal variability in running correlations is significantly more variable than can be expected due to stochasticity. This result holds for window widths of 15, 21, and 31 yr and also for high-pass-filtered streamflow.

TABLE 1. Seasonal breakdown of Kelani streamflow at Glencourse station for 1948–93. The correlation of rainfall with Niño-3.4 and rainfall for the same period is also shown. Correlations that are significant at 95% are shown in bold.

Season characteristic	JFM	AMJ	JAS	OND	Annual
Mean streamflow (MCM)	319	909	820	965	3017
Std dev of streamflow (MCM)	128	283	269	274	528
Correlation with Niño-3.4					
(1925–95)	0.06	−0.04	**−0.33**	**0.24**	**−0.17**
(1925–50)	0.23	**0.38**	**−0.39**	0.28	0.31
(1951–75)	0.28	−0.03	−0.11	0.03	−0.33
(1976–95)	−0.34	**−0.43**	**−0.62**	**0.42**	**−0.43**

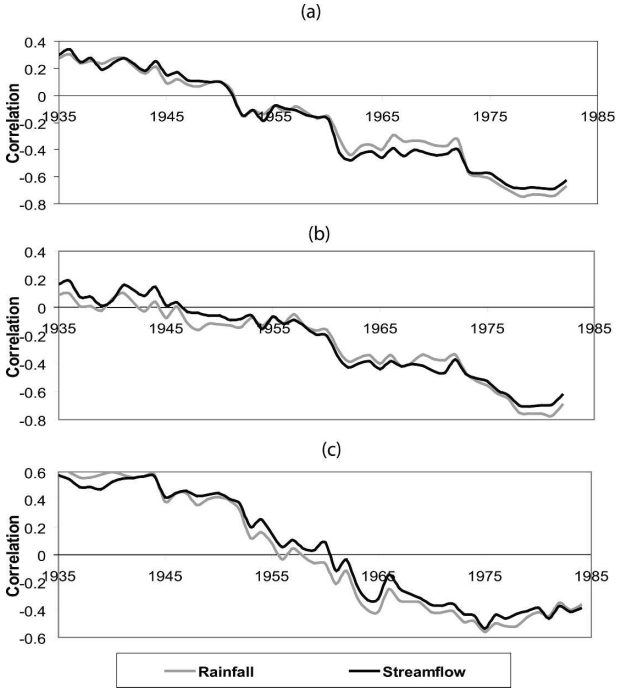

FIG. 5. (a) The 21-yr sliding window correlation between the concurrent January–September catchment streamflow (rainfall) and Niño-3.4. (b) As in (a) but with the streamflow and rainfall high-pass filtered. (c) The correlation between December Niño-3.4 and January–September streamflow and rainfall.

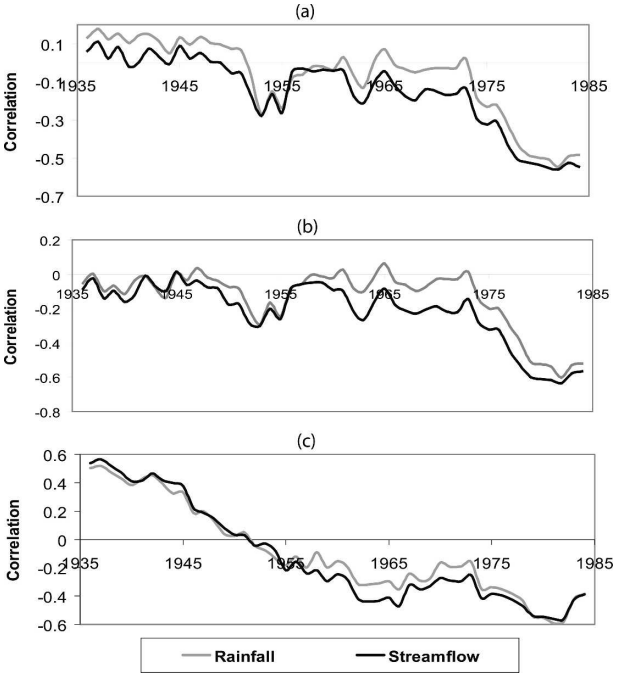

FIG. 6. (a) The 21-yr sliding window correlation between the concurrent April–September streamflow, catchment rainfall, and Niño-3.4. (b) As in (a) but with rainfall and streamflow high-pass filtered. (c) The correlation of January–September streamflow and rainfall with previous Decembers' Niño-3.4.

c. *ENSO–rainfall relationships*

To verify the decadal variability found in the ENSO–streamflow relationship with independent data, a parallel analysis was carried out with rainfall records. A sliding window correlation between January–September and April–September rainfall and Niño-3.4 is shown in Figs. 5 and 6. It too shows a transition in the 1950s for the January–September season with the transition delayed till 1970 for the April–September season.

In recent decades, the ENSO–rainfall relationship has actually strengthened, reaching −0.45 for January–September, −0.32 for April–September, and −0.44 for July–September.

The more abrupt strengthening in the April–September correlation with ENSO in relation to the gentler drop in correlation during the January–September period was replicated with the two rainfall indices and the high-pass-filtered versions of these data.

d. *Differences between January–September and April–September correlations*

To isolate the cause of this difference, we computed the running window correlations of January–March, April–June, and July–September Niño-3.4 and streamflow indices separately (not shown). The positive correlation between streamflow and Niño-3.4 for January–March is sustained at around +0.3 until 1970 and thereafter it turns negative at around −0.3 through the 1970s. Thus the difference in the decadal modulation due to ENSO is likely due to differences in the changing climate dynamics in January–March with respect to the April–September season. The recent Indian Ocean warming may be implicated as it was found to affect the regional climate during the January–March season (Hoerling et al. 2004).

e. *Streamflow predictions based on ENSO*

The relationships between ENSO and streamflow in the recent period as shown in Figs. 5 and 6 may be leveraged to provide predictions. The contemporaneous relationships between Niño-3.4 and streamflow and rainfall can be used along with ENSO predictions that are now available to obtain streamflow predictions at the start of each season. The skill of such ENSO predictions will be better for the April–September season as it is after the transitional phase of the ENSO phenomenon in the boreal spring.

A more practical option is to use the lag–lead relationships between streamflow and ENSO indices. The

correlation between the Niño-3.4 index in December and the subsequent January–September streamflow is −0.4 (significant at the 95th percentile) from 1975 to 1995. The predictability obtained for the January–September period is notwithstanding the transitional phase of the ENSO cycle in the boreal spring. We also report on the April–September season, which is important as it is the water-constrained *Yala* agricultural season. The correlation between the Niño-3.4 index in March and the subsequent *Yala* streamflow strengthens from −0.08 from 1949 to 1970 to −0.48 (significant at the 99th percentile) from 1970 to 2000. Thus the predictability is improved as spring passes.

ENSO streamflow correlations are just about significant with Niño-3.4 in the month prior to the season to be predicted. The correlation for the April–September season is slightly greater than that of January–September. A prediction scheme may have to contend with a decline in skill in a cross-validated model. Given the decadal variability, it shall be prudent to continuously assess the skill of any prediction scheme.

f. Relationships with large-scale circulation

Global circulation fields are available from 1948 onward from the NCEP–NCAR analysis. We examined the changes between the early and late halves of the record to evaluate for significant decadal changes. We constructed composites of the April–September vertical velocity for the 600-mb layer, which is a representative value of the maximum in a standard atmosphere. In comparison with the early period, there is enhanced subsidence over Sri Lanka during more recent El Niño episodes (Fig. 7). This enhanced subsidence is consistent with the increased diminution of rainfall and streamflow during more recent El Niño episodes.

We also constructed composites of the April–September 200-hPa velocity potential anomaly fields for the ENSO warm episodes for the 1948 to 1973 and 1974 to 1998 periods (not shown). In comparison with the early period, the coverage and magnitude of the region of positive velocity potential over the western Indian Ocean has been enhanced in the late period suggesting relatively enhanced subsidence in the large-scale features.

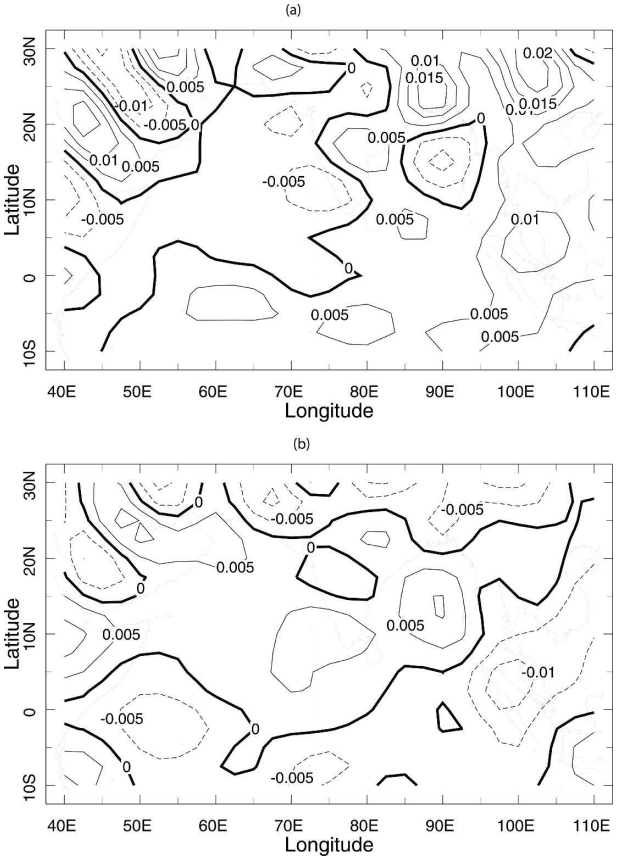

FIG. 7. The vertical velocity composites (Pa s^{-1}) for April–September during El Niño episodes at 600 mb for (a) 1958–73 (1953, 1957, 1958, 1963, 1965, 1969, 1972) and (b) 1974–98 (1976, 1977, 1982, 1986, 1987, 1991, 1992, 1993, 1994, 1997).

4. Conclusions

This work has shown that ENSO has significant negative correlation with the Kelani streamflow during January–September and April–September seasons after around 1960. There has been a transition from a near-zero correlation in the early part of the record to a 99% level of significance for the January–September season and 95% level of significance for the April–September season. This transition occurred between 1950 and 1970. The change in correlation could not be attributed to stochasticity alone. The relationship of seasonal streamflow has become salient even with Niño-3.4 observed prior to the January–September and April–September seasons.

The strengthening relationship with ENSO was retained even after the low-frequency variability in the rainfall and streamflow signals were removed. These results were confirmed by analyzing the decadal modulation of the ENSO correlation with rainfall. The transition that occurred during the 1950–70s is reminiscent of an epochal shift.

Examination of large-scale circulation features shows that subsidence over the region during El Niño episodes has been enhanced after the mid-1970s, which is consistent with the strengthening ENSO–rainfall relationships reported here.

5. Discussion

Epochal changes in ENSO attributes such as its variance and its relationship with other climatic features has been reported by several workers (e.g., Rasmusson et al. 1994; Suppiah 1996; Kestin et al. 1998; Kumar et al. 1999a; Hoerling et al. 2004) and appears to be a systemwide phenomenon that is yet to be comprehensively understood. The interdecadal modulation of the ENSO teleconnection in North America has been characterized by Gershunov and Barnett (1998).

The weakening of the ENSO–monsoon relationship over India but not over Sri Lanka is intriguing. Sri Lanka is located closer to the boundary demarcating regions of anomalous ascent and anomalous descent during El Niño episodes. There is considerable evidence of interdecadal modulation of SST, velocity potential, and ENSO influence in the Indian Ocean (Allan et al. 1995). It is quite plausible therefore that there have been geographic and seasonal shifts in the influence of ENSO since the 1950s.

As the linkage between ENSO and January–September and April–September rainfall has been sustained for the last three decades, the potential for the use of ENSO based precursors for streamflow prediction is retained. Investigations of other potential climatic precursors for streamflow such as Indian Ocean conditions (Zubair et al. 2003) and Eurasian snow cover on streamflow and rainfall should help to improve any predictions.

The reversal of the ENSO influence may explain the loss of salience in the El Niño–malaria relationship since 1945. In the wet part of Sri Lanka, which includes the Kelani basin, mosquito breeding is likely due to pooling in river margins. River margin pooling occurs due to abrupt rises and drops in river levels. However, the propensity for such fluctuations with El Niño events is no longer what it was prior to the 1950s as the ENSO–streamflow relationship has undergone an inversion since then.

Acknowledgments. Data used in this study were obtained from the Departments of Irrigation and Meteorology in Sri Lanka. Upamala Tennakoon and Zeenas Yahiya assisted with the figures and revisions. Much of the climatic analysis is based upon work conducted with Chet Ropelewski. The comments of the reviewers and editor helped improve the manuscript tremendously. This paper is funded in part by a grant/cooperative agreement from the National Oceanic and Atmospheric Administration, NA050AR4311004, and also a grant from NOAA, NA03OAR4310161. The views expressed herein are those of the authors and do not necessarily reflect the views of NOAA or any of its subagencies.

REFERENCES

Allan, R. J., J. A. Lindesay, and C. J. C. Reason, 1995: Multidecadal variability in the climate system over the Indian Ocean region during the austral summer. *J. Climate,* **8,** 1853–1873.

——, ——, and D. Parker, 1996: *El Niño/Southern Oscillation and Climate Variability*. CSIRO Press, 405 pp.

Ashok, K., Z. Guan, and T. Yamagata, 2001: Impact of the Indian Ocean Dipole on the decadal relationship between Indian monsoon rainfall and ENSO. *Geophys. Res. Lett.,* **28,** 4499–4502.

Bouma, M. J., and H. J. Van der Kaay, 1996: The El Niño Southern Oscillation and the historic malaria epidemics on the Indian subcontinent and Sri Lanka: An early warning system for future epidemics? *Tropical Medicine and International Health,* Vol. 1, No. 1, Blackwell, 86–96.

Chang, C. P., P. Harr, and J. Ju, 2001: Possible roles of Atlantic circulations on the weakening Indian monsoon rainfall–ENSO relationship. *J. Climate,* **14,** 2376–2380.

Dettinger, M. D., D. R. Cayan, G. J. McCabe, and J. A. Marengo, 2000: Multiscale streamflow variability associated with El Niño/Southern Oscillation. *El Niño and the Southern Oscillation: Multiscale Variability and Global and Regional Impacts,* H. F. Diaz and V. Markgraf, Eds., Cambridge University Press, 113–146.

Gershunov, A., and T. P. Barnett, 1998: Interdecadal modulation of ENSO teleconnections. *Bull. Amer. Meteor. Soc.,* **79,** 2715–2725.

——, N. Schneider, and T. P. Barnett, 2001: Low-frequency modulation of the ENSO–monsoon relationship: Signal or noise? *J. Climate,* **14,** 2486–2492.

Hanley, D. E., M. A. Bourassa, J. J. O'Brien, S. R. Smith, and E. R. Spade, 2003: A quantitative evaluation of ENSO indices. *J. Climate,* **16,** 1249–1258.

Hoerling, M. P., J. W. Hurrell, T. Xu, G. T. Bates, and A. Phillips, 2004: Twentieth century North Atlantic climate change. Part II: Understanding the effect of Indian Ocean warming. *Climate Dyn.,* **23,** 391–405.

Janowiak, J. E., and P. Xie, 1999: CAMS–OPI: A global satellite–rain gauge merged product for real-time precipitation monitoring applications. *J. Climate,* **12,** 3335–3342.

Kaplan, A., M. A. Cane, Y. Kushnir, A. C. Clement, M. B. Blumenthal, and B. Rajagopalan, 1998: Analyses of global sea surface temperature: 1856–1991. *J. Geophys. Res.,* **103,** 18 567–18 589.

Kestin, T. S., D. J. Karoly, J. I. Yano, and A. Rayner, 1998: Time–frequency variability of ENSO and stochastic simulations. *J. Climate,* **11,** 2258–2272.

Kistler, R., and Coauthors, 2001: The NCEP–NCAR 50-Year Reanalysis: Monthly means CD-ROM and documentation. *Bull. Amer. Meteor. Soc.,* **82,** 247–267.

Krishnamurthy, V., and B. N. Goswami, 2000: Indian monsoon–ENSO relationship on interdecadal timescale. *J. Climate,* **13,** 579–585.

Kumar, K. K., R. Kleeman, M. A. Cane, and B. Rajagopalan, 1999a: Epochal changes in Indian monsoon–ENSO precursors. *Geophys. Res. Lett.,* **26,** 75–78.

——, B. Rajagopalan, and M. A. Cane, 1999b: On the weakening relationship between the Indian monsoon and ENSO. *Science,* **284,** 2156–2159.

Mehta, V. M., and K. M. Lau, 1997: Influence of solar irradiance

on the Indian monsoon–ENSO relationship on interdecadal time scales. *Geophys. Res. Lett.,* **24,** 159–162.

Oppenheim, A. V., and R. W. Schafer, 1975: *Digital Signal Processing*. Prentice-Hall, 598 pp.

Press, W. H., S. A. Teukolosky, W. T. Vetterling, and B. P. Flannery, 1992: *Numerical Recipes in Fortran*. Cambridge University Press, 963 pp.

Puvaneswaran, K. M., and D. A. Smithson, 1993: Controls on the precipitation distribution in Sri Lanka. *Theor. Appl. Climatol.,* **47,** 105–115.

Rasmusson, E. M., and T. H. Carpenter, 1983: The relationship between eastern equatorial Pacific sea surface temperature and rainfall over India and Sri Lanka. *Mon. Wea. Rev.,* **110,** 354–384.

——, X. L. Wang, and C. F. Ropelewski, 1994: Secular variability of the ENSO cycle. *Decade to Century Time Scales of Natural Climate Variability,* D. G. Martinson et al., Eds., Academic Press, 458–471.

Ropelewski, C. F., and M. S. Halpert, 1987: Global and regional scale precipitation patterns associated with the El Niño/Southern Oscillation. *Mon. Wea. Rev.,* **115,** 1606–1626.

Soman, M. K., and J. M. Slingo, 1997: Sensitivity of the Asian summer monsoon to aspects of the sea surface temperature anomalies in the tropical Pacific Ocean. *Quart. J. Roy. Meteor. Soc.,* **123,** 309–336.

Suppiah, R., 1996: Spatial and temporal variations in the relationships between the Southern Oscillation phenomenon and the rainfall of Sri Lanka. *Int. J. Climatol.,* **16,** 1391–1407.

Wang, G., and E. A. B. Eltahir, 1999: Use of ENSO information in medium and long-range forecasting of Nile floods. *J. Climate,* **12,** 1726–1737.

Whitaker, D. W., S. A. Wasimi, and S. Islam, 2001: The El Niño Southern Oscillation and long-range forecasting of the flows in the Ganges. *Int. J. Climatol.,* **21,** 77–87.

Yaffee, R., and M. McGee, 2000: *Time Series Analysis and Forecasting*. Academic Press, 496 pp.

Zubair, L., 2002a: El-Niño–Southern Oscillation influences on rice production in Sri Lanka. *Int. J. Climatol.,* **22,** 242–250.

——, 2002b: Diurnal and seasonal variations in surface winds at Sita Eliya, Sri Lanka. *Theor. Appl. Climatol.,* **71,** 119–127.

——, 2004: *Weather and Climate of Sri Lanka and Impacts and Adaptation: A Reference Guide.* Natural Resources Management Services, 116 pp.

——, S. C. Rao, and T. Yamagata, 2003: Modulation of Sri Lanka rainfall by the Indian Ocean Dipole. *Geophys. Res. Lett.,* **30,** 1063, doi:10.1029/2002GL015639.